Laser scanning lithography for surface micropatterning on hydrogels

Mariah S. Hahn, PhD
Jordan S. Miller
Jennifer L. West, PhD
Department of Bioengineering, Rice University

Introduction

Techniques that control the spatial presentation of moieties such as cell adhesion peptides on surfaces are important for the advancement of tissue engineering, the elucidation of fundamental tissue structure-function relationships, and the formation of immobilized cell and protein arrays for biotechnology.[1] Cell and protein patterns have previously been created using a range of methods, including photolithography[2, 3] and soft lithographic approaches such as microcontact printing,[4] microfluidic patterning,[5, 6] and micromolding.[7, 8] The patterned substrates have generally been modified silicon or glass,[9, 10] whereas surface patterning of deformable, solvated substrates has not received a similar degree of attention. High fidelity patterning of deformable, solvated substrates is challenging, particularly since many commonly used patterning techniques cannot be readily applied. For example, microcontact printing is generally not applicable to such substrates due to lateral diffusion of the patterned molecule when the inked stamp comes into contact with the solvated substrate. Given the importance of deformable, solvated substrates, such as hydrogels, as scaffolds for soft tissue engineering applications, development of methods for direct, high fidelity surface patterning of these substrates is desirable.

Poly(ethylene glycol) (PEG)-based hydrogels are biocompatible and intrinsically resistant to protein adsorption and cell adhesion, thus providing a biological "blank slate" upon which desired biofunctionality can be built.[11] Acrylate-terminated PEG macromers undergo rapid polymerization upon exposure to UV or visible light when in the presence of appropriate photoinitiators.[12, 13] This work develops confocal-based laser scanning lithography (LSL)[14, 15] for 2D and 3D surface patterning of hydrated, photoactive PEG-based hydrogel substrates.

Experimental

Cell maintenance

Human dermal fibroblasts (HDFs, Cambrex) were maintained in DMEM supplemented with 10% FBS, 2 mM L-glutamine, 1000 U/L penicillin, and 100 mg/L streptomycin at 37 °C/5% CO_2. Cells were used at passages 7-12. All cell culture reagents were obtained from Sigma.

Fluorescently-labeled PEG-peptide synthesis

Peptide RGDS (American Peptide) was conjugated to PEG (3400 MW) by reaction with ACRL-PEG-NHS (Nektar) at a 1:1 molar ratio for 2 h in 50 mM sodium bicarbonate buffer, pH 8.5. Alexa Fluor 488 carboxylic acid, tetrafluorophenyl (TFP) ester (Molecular Probes) was then added to the ACRL-PEG-RGDS reaction mixture at approximately 10 moles dye per mole PEG-peptide and allowed to react for 1 h at room temperature.

Photopolymerization of PEGDA hydrogels

A solution was prepared containing 10% (w/v) 3400MW PEGDA and 1.5% (v/v) triethanolamine (TEOA) in HEPES buffered saline (pH 7.4, HBS), 0.4% (v/v) N-vinylpyrrolidone (NVP), and 100 μM eosin Y (a biocompatible visible light photoinitiator). This solution was polymerized between two glass plates separated by 0.5 mm spacers by exposure to high intensity white light.

Laser scanning lithography

A schematic of the patterning process is shown in Fig. 1. Briefly, the upper surface of a pre-swelled PEGDA hydrogel was positioned at the focal plane of a 10X Plan-Apochromat objective (NA 0.45) attached to a LSM 510 META confocal microscope (Zeiss). "Virtual masks" were then created by drawing "regions of interest" (ROIs), i.e., regions where laser irradiation is desired, using standard confocal LSM software. The LSM software converts these ROIs into instructions that dictate which pixel locations the laser shutter is opened during an irradiation cycle.

1. Position photoactive hydrogel or substrate. Create a virtual mask using the ROI functionality.

2. Spread fluorescent acrylol-PEG-peptide onto substrate surface. Begin irradiation cycle in which the laser line is scanned unidirectionally across the gel, with light only being applied in ROI boundaries.

3. PEG-peptide crosslinks to substrate only in irradiated regions. Bound peptide can be visualized by fluorescence. Pattern arrays can be created using a motorized stage.
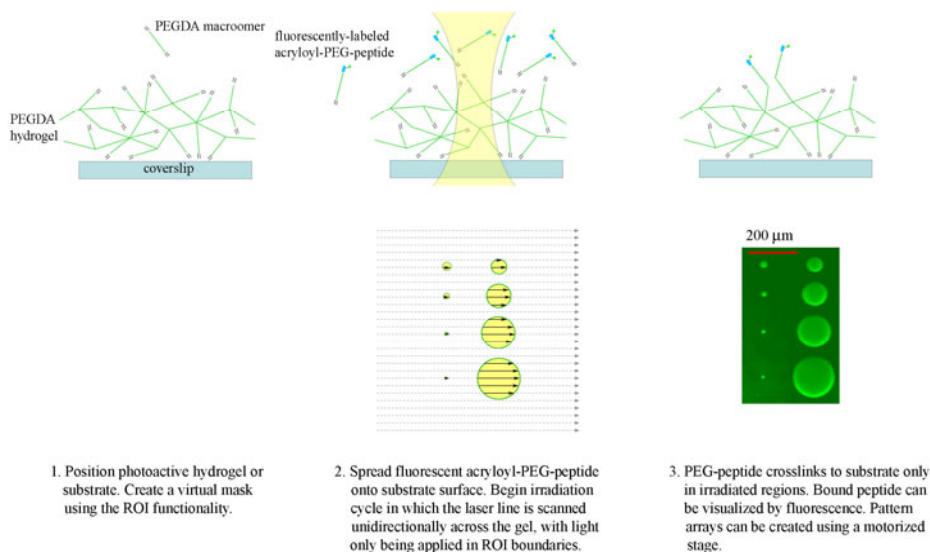
Figure 1. Schematic of surface patterning of photoactive substrates using LSL, with PEGDA hydrogels used as the model substrate. The upper row of images illustrates the patterning mechanism at the molecular level, transverse to the plane of the substrate surface. The bottom row of images depicts the patterning methodology at the macroscopic level, parallel to the substrate surface. The fluorescence image in the lower right hand corner is of an actual hydrogel patterned with fluorescent ACRL-PEG-RGDS and demonstrates that features down to ~5 μm in size can be produced.

Two dimensional surface patterns

A thin layer of fluorescently-labeled ACRL-PEG-peptide (30 μmol/mL) dissolved in HBS/TEOA containing 0.4% NVP and 100 μM eosin Y was spread onto the surface of the PEGDA gel. For the fluorescence pattern images in Fig. 1, Fig. 2a, and Fig. 3, patterning was carried out using an irradiation cycle in which a 514 nm Argon ion laser line was unidirectionally scanned across the specified ROIs at 0.25 mW/μm^2 and 50 μsec/μm^2. Unbound ACRL-PEG-peptide was rinsed away with sterile PBS. For the gradient patterns in Fig. 2b-c, 514 Argon ion laser power was maintained at 0.25 mW/μm^2; however, a range of irradiation times were used across ROIs, with a minimum exposure time of 0.4 μsec/μm^2. Successful patterning of the fluorescently-labeled peptides was confirmed by visualization under fluorescence (Zeiss LSM 510 META). The bioactivity of patterned cell adhesion

peptide RGDS was evaluated by seeding HDFs onto patterned hydrogel surfaces and examining cell adhesion via DIC imaging (Zeiss LSM 510 META) at days 1 and 4.

Three dimensional surface patterns

A thin layer of 0.2 g/mL 600 MW PEGDA (Sarcomer) dissolved in HBS/TEOA containing 0.4% NVP and 100 μM eosin Y was spread onto the surface of the PEGDA gel. Patterning was carried out using an irradiation cycle in which a 514 nm Argon ion laser line was unidirectionally scanned across the specified ROIs at 0.25 mW/μm^2 and 50 $\mu sec/\mu m^2$. Unbound ACRL-PEG-peptide was rinsed away with sterile PBS, and patterning was confirmed through DIC imaging (Zeiss LSM 510 META).

Results

A wide range of features, including free-form objects (Fig. 2a) and patterns down to at least 5 μm in size (Fig. 1), can be patterned with high fidelity on the hydrated gel surfaces using this procedure. Since the surface density of bound ACRL-PEG-peptide in the irradiated ROIs is dependent on user-specified irradiation exposure time and intensity, the surface peptide concentration can be spatially controlled by the user, allowing for complex 2D concentration gradients to be formed (Fig. 2b-c).
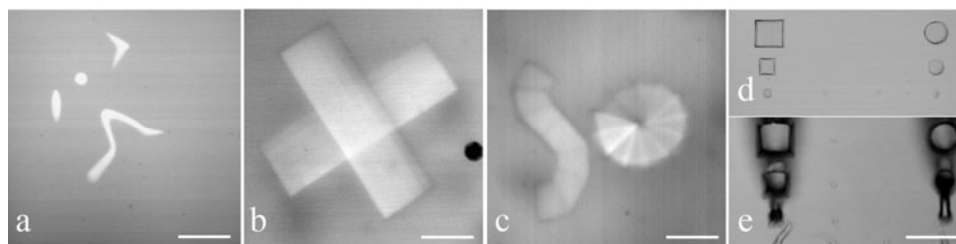

Figure 2. Demonstration of the versatility of LSL hydrogel surface patterning. a.) A grayscale fluorescence image of free-form ROIs patterned with fluorescently labeled ACRL-PEG-RGDS. b-c.) Grayscale fluorescence images of 2D concentration gradients of ACRL-PEG-RGDS formed by varying irradiation exposure times across ROIs. Note the flexibility in orientation of the patterned regions. d, e.) DIC images of 3D patterns formed by including PEGDA in the precursor solution. Features in (d) are ~ 4 μm in height, while those in (e) are ~ 20 μm in height. Note the axial variation in feature size in (e) due to laser beam diffraction from its focal point. Scale bars = 200 μm.

As shown schematically in Fig. 1, monolayer surface patterns are created when the precursor solution contains only monoacrylate-derivatized PEG-peptides. However, since confocal irradiation is not limited to the laser beam focal plane, irradiation can result in 3D surface patterns if diacrylate-derivatized PEG macromers are added to the precursor solution (Fig. 2d-e). Features ranging from 0 to roughly 5 μm in height can be formed with low axial distortion (Fig. 2d), although the fidelity of the patterned features is reduced as the thickness of the precursor solution layer increases due to laser beam diffraction from its focal point (features ~4 μm height, Fig. 2d vs features ~20 μm height, Fig. 2e). Three dimensional microstructures have been used to provide topographical cues to control cellular organization.[18, 19]

To evaluate the feasibility of using peptide-patterned PEGDA hydrogels for spatially controlled cell attachment, human dermal fibroblasts (HDFs) were seeded onto patterned monolayers of ACRL-PEG-RGDS. As expected, cells selectively adhered to hydrogel regions patterned with the cell adhesive peptide RGDS (Fig. 3).
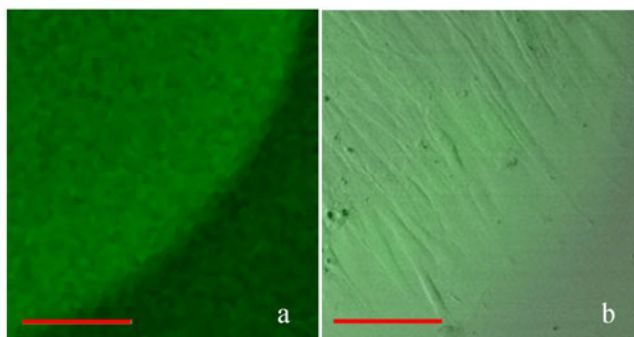
Figure 3. Cell adhesion on LSL-patterned PEGDA hydrogel substrates. a.) Fluorescence image of an ACRL-PEG-RGDS surface pattern. b.) DIC image of the confluent HDF monolayer onto the corresponding fluorescence pattern image (a). Note that the HDFs are localized within the boundaries of the ACRL-PEG-RGDS patterned region. Scale bars = 100 μm.

Discussion

A versatile confocal-based laser scanning lithographic method for controlled, high fidelity surface patterning of deformable, solvated, photoactive substrates has been presented. This method for immobilizing biomolecules in 2D and 3D can be applied to any optically clear, photoactive substrate, whether rigid or deformable. Since user-defined "virtual masks" are used to spatially control laser irradiation during pattern generation, the need for conventional photolithographic masks and for a clean room is eliminated. Since the created patterns are covalently linked to the substrate surface, the patterns are mechanically and chemically stable.

In the present work, the surface properties of deformable, biocompatible PEGDA hydrogels have been modified in a controlled manner using LSL, with pattern feature sizes down to at least 5 μm being achievable. HDFs have been shown to selectively bind to regions patterned with appropriate cell adhesive peptides and to retain their spatial localization in culture. Complex 2D concentration gradients of patterned peptides have been generated via user alteration of irradiation exposure levels across ROIs, a degree of spatial control over irradiation not readily achieved using conventional photolithographic masks. Three dimensional structures of varying heights have also been created using LSL, although pattern fidelity was maintained only for features under roughly 5 μm in height due to laser beam diffraction from its focal point. Since both 2D and 3D structures can be formed, LSL should allow for the controlled study of the separate effects of pattern 2D geometry versus pattern topography on cell behavior. The flexibility offered by this technique in terms of feature topography, bound peptide concentration, and substrate type is particularly desirable in tissue engineering applications, where patterning often seeks to mimic the complex organization of soft tissues. Controlled functionalization of surfaces should allow for increased insight into cell behavior, cell-cell interactions, and cell-biomaterial interactions and for the elucidation of fundamental structure-function relationships of tissues.

References

1. T. Chovan, A. Guttman, *Trends in Biotechnology* **2002**, *20*, 116.
2. D. Ryan, B. A. Parviz, V. Linder, V. Semetey, S. K. Sia, J. Su, M. Mrksich, G. M. Whitesides, *Langmuir* **2004**, *20*, 9080.

3.   C. B. Herbert, T. L. McLernon, C. L. Hypolite, D. N. Adams, L. Pikus, C.-C. Huang, G. B. Fields, P. C. Letourneau, M. D. Distefano, W.-S. Hu, *Chemistry and Biology* **1997**, *4*, 731.
4.   C. S. Chen, M. Mrksich, S. Huang, G. M. Whitesides, D. E. Ingber, *Biotechnol. Prog.* **1998**, *14*, 356.
5.   S. Takayama, J. C. McDonald, E. Ostuni, M. N. Liang, P. J. A. Kenis, R. F. Ismagilov, G. M. Whitesides, *Proc. Natl. Acad. Sci. U.S.A* **1999**, *96*, 5545.
6.   E. Delamarche, A. Bernard, H. Schmid, B. Michel, H. Biebuyck, *Science* **1998**, *276*, 779.
7.   K. Y. Suh, J. Seong, A. Khademhosseini, P. E. Laibinis, R. Langer, *Biomaterials* **2004**, *25*, 557.
8.   A. Khademhosseini, S. Jon, K. Y. Suh, T.-N. T. Tran, G. Eng, J. Yeh, J. Seong, R. Langer, *Adv. Mater.* **2003**, *15*, 1995.
9.   Y. Xia, G. M. Whitesides, *Angew Chem Int Ed* **1998**, *37*, 550.
10.   R. S. Kane, S. Takayama, E. Ostuni, D. E. Ingber, G. M. Whitesides, *Biomaterials* **1999**, *20*, 2363.
11.   W. R. Gombotz, G. H. Wang, T. A. Horbett, A. S. Hoffman, *Journal of Biomedical Materials Research* **1991**, *25*, 1547.
12.   J. L. West, J. A. Hubbell, *Reactive Polymers* **1995**, *25*, 139.
13.   J. L. Hill-West, S. M. Chowdhury, M. J. Slepian, J. A. Hubbell, *Proceedings of the National Academy of Science U.S.A.* **1994**, *91*, 5967.
14.   C. Rensch, S. Hell, M. V. Schickfus, S. Hunklinger, *Applied Optics* **1989**, *28*, 3754.
15.   L. P. Ghislain, V. B. C. Elings, K.B., S. R. Manalis, S. C. Minne, K. Wilder, G. S. Kino, C. F. Quate, *Applied Physics Letters* **1999**, *74*, 501.
16.   Y. Ito, M. Hayashi, Y. Imanishi, *J. Biomater. Sci.-Polym. Ed.* **2001**, *12*, 367.
17.   G. Chen, Y. Ito, *Biomaterials* **2001**, *22*, 2453.
18.   S. Sarkar, D. M., P. Rourke, T. A. Desai, J. Y. Wong, *Acta Biomaterialia* **2005**, *1*, 93.
19.   R. G. Flemming, C. J. Murphy, G. A. Abrams, S. L. Goodman, P. F. Nealey, *Biomaterials* **1999**, *20*, 573.